



One-pot Preparation of a Novel CO-Releasing Material based on a CO-Releasing Molecule@Metal-Organic Framework System

Received 00th January 20xx,
Accepted 00th January 20xx

F. J. Carmona,^a S. Rojas,^a C. C. Romão,^{bc} J. A. R. Navarro,^a E. Barea,^{*a} and C. R. Maldonado^{*a}

DOI: 10.1039/x0xx00000x

www.rsc.org/

A novel CO releasing material has been prepared by a one-pot synthesis-encapsulation strategy using the hierarchical metal organic framework [Zn₂(dhtp)] (dhtp = 2,5-dihydroxyterephthalate) as a host of the photoactivable molybdenum tricarbonyl complex [Mo(CNCMe₂CO₂H)₃(CO)₃].

CO is currently considered a potential therapeutic agent against various disease models, even though, its reputation as toxic gas.¹ In fact, inhalation of CO, the simplest way to exogenously administrate this molecule, has entered multiple clinical trials.² However, this strategy lacks specificity as the biodistribution of this therapeutic gas depends on tissues partition coefficients.³ In this context, other approaches are currently under development with the aim of achieving a more efficient and specific CO therapeutic administration. For example, "CO-releasing molecules" (CORMs), which are generally metal carbonyl complexes, have excellent prospects as pro-drugs capable of delivering CO in response to a stimulus (e.g. light, pH change, etc.).⁴ However, despite their promising characteristics, these molecules have some disadvantages that prevent their clinical application, such as *i)* low solubility and/or stability in physiological media, *ii)* potential toxicity of their metal decarbonylation fragments, and/or *iii)* fast CO release upon stimulation.⁵ Therefore, more sophisticated strategies able to overcome these drawbacks are needed. In this sense, Shiller *et al.* introduced the concept of CO-releasing materials (CORMAs) in 2014.⁶ CORMAs can be defined as solid CO storage materials able to deliver this gas in a triggered manner. Thus, one of the most versatile strategies to design new CORMAs consists in the combination of a CO releasing molecule with an appropriate platform acting as a

biocompatible vehicle. Up to the date, few examples of a wide variety of materials have been investigated for this application, comprising organic polymers, proteins, dendrimers, inorganic nanoparticles, and inorganic porous matrixes.^{7,8} Regarding the later, the use of these compounds, namely mesoporous silicas and metal organic frameworks (MOFs), may add some advantages to the resulting CORMAs. In fact, the presence of large pore volumes can lead to high payloads, while the potentially toxic metal-coligand fragments are expected to remain trapped inside the pores.

The first example of a CORMA based on a mesoporous silica encapsulating a CORM was reported by Mascharak and col.⁹ On the other hand, Metzler-Nolte *et al.* prepared the first CO-delivery system using a MOF as a platform.¹⁰ In this case, they took advantage of the unsaturated coordination sites of MIL-88B-Fe and its amine derivative, to reversibly capture carbon monoxide and, later, deliver it by simple degradation of the matrixes. Afterwards, to the best of our knowledge, the first example of a CORM@MOF system was published by our group using a cation exchange methodology.¹¹ Despite the success of this encapsulation strategy and the possibility of light triggering, the scarce stability of the resulting hybrid material in physiological conditions led to the complete leaching of the CORM in a short timeframe. More recently, Furukawa *et al.* have smartly designed a covalently attached CORM@MOF system by embedding a photoactive manganese complex into a robust Zr(IV)-MOF. In this case, CO delivery was monitored in the solid state.¹²

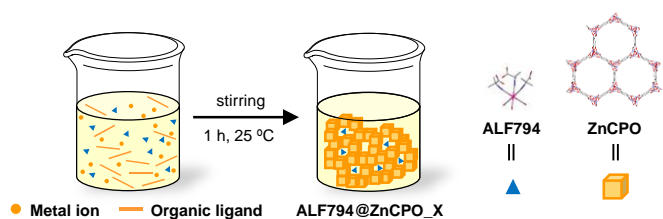
Taking into account all the above, in this communication, we report the one-pot synthesis of a new CORM@MOF system by incorporating the CORM [Mo(CNCMe₂CO₂H)₃(CO)₃] (ALF794)¹³ into the textural mesopores of the hierarchical structure of [Zn₂(dhtp)] (dhtp = 2,5-dihydroxyterephthalate) (h-ZnCPO)¹⁴ (Scheme 1). In addition, both stability and CO-delivery kinetics studies of the resulting hybrid material have been evaluated in simulated physiological conditions, revealing a scarce degradation of the system in such conditions as well as the retention of most of the decarbonylation fragments after CO release.

^a Department of Inorganic Chemistry, University of Granada, Av. Fuentenueva S/N, 18071 Granada, Spain.

^b Instituto de Tecnologia Química e Biológica da Universidade Nova de Lisboa, Av. da República, EAN, 2780-157 Oeiras, Portugal

^c Alfama Ltd., Instituto de Biologia Experimental e Tecnológica, IBET, Av. da República, EAN, 2780-157 Oeiras, Portugal.

†Electronic Supplementary Information (ESI) available: Experimental methods, EA, SEM and TEM images, chemical stability studies (IR and XRPD) and leaching tests (ICP-OES). See DOI: 10.1039/x0xx00000x



Scheme 1. One-pot encapsulation strategy of ALF794 into the hierarchical porous matrix h-ZnCPO.

The selected molybdenum complex for this work, $[\text{Mo}(\text{CNCMe}_2\text{CO}_2\text{H})_3(\text{CO})_3]$ (ALF794), is an air-water stable photoCORM. *In vivo* studies have also revealed that this compound shows low toxicity in mice ($\text{LD}_{50} > 300 \text{ mg Kg}^{-1}$)¹⁵ with preferential CO release in the liver proving its efficacy against induced acute liver injury.¹³ On the other hand, $[\text{Zn}_2(\text{dhtp})]$ (dhtp = 2,5-dihydroxyterephthalate) (ZnCPO) is a suitable candidate for biomedical applications due to the low toxicity of Zn^{2+} metal ions (oral $\text{LD}_{50} \sim 100\text{--}600 \text{ mg Kg}^{-1}$ in rats). In addition, the porous structure of this MOF shows 1D hexagonal channels along the *c* axis available for the encapsulation of guest molecules. However, the microporous nature of ZnCPO with a pore aperture of $1.0 \times 1.4 \text{ nm}$ ¹⁶ may hamper the diffusion of bulky molecules, such as ALF794 (ca. 1.3 nm).¹³ Indeed, all attempts to incorporate ALF794 in this microporous MOF did not succeed. For this reason, we decided to use the novel “perturbation-assisted nanofusion method” (PNF)^{14,17} in order to obtain a hierarchical ZnCPO structure with micro- and mesopores. This synthetic strategy allows the formation of nanoparticles aggregates that originate randomly distributed textural mesopores where large guest molecules (e.g. ALF794) can be successfully encapsulated. Thus, following this methodology we obtained a hierarchical material (h-ZnCPO) with similar features than the previously reported by Dai *et al.* (see ESI).¹⁴ In order to evaluate the potential of this matrix as vehicle for the development of new CORMAs, we first studied its chemical stability in the physiological buffer HEPES (10 mM, pH = 7.4). This MOF demonstrated a high chemical stability after incubation in HEPES at 37 °C for 6 hours. Indeed, no significant changes neither in infrared spectra (IR) nor in X-ray powder diffractograms (XRPD) were observed (Fig. S1).

In view of these results, and taking into account that h-ZnCPO is synthesized under mild conditions (RT and stirring), we decided to load ALF794 during the preparation of the MOF (Scheme 1). This one-pot synthesis-encapsulation strategy would allow a rapid and efficient encapsulation of the CO-prodrug, as the number of required steps, energy requirements, and operation/manipulation time could be minimized, as it has been previously reported for other systems.^{18,19} Likewise, the risk of CORM degradation or accidental activation would decrease. The one-pot reaction was performed in darkness and at room temperature by stirring vigorously a DMF solution containing $\text{Zn}(\text{AcO})_2 \cdot 2\text{H}_2\text{O}$, 2,5-dihydroxyterephthalic acid and the appropriate amount of ALF794. In order to optimize the efficiency of the process, we

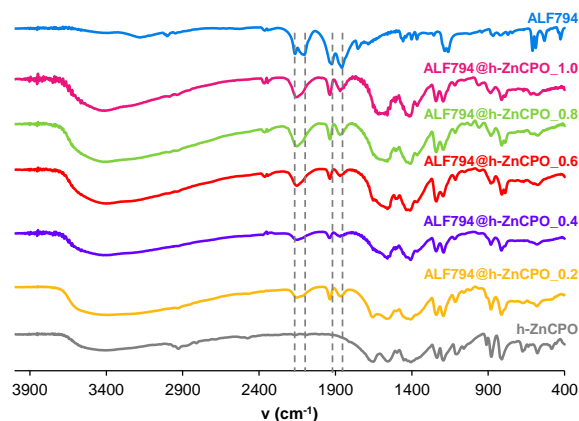


Fig. 1 IR spectra of ALF794, h-ZnCPO and the corresponding hybrid materials ALF794@h-ZnCPO_x (x = CORM/ Zn^{2+} molar ratio used during the synthesis).

screened different CORM/ Zn^{2+} molar ratios (x = 0.2, 0.4, 0.6, 0.8, and 1.0), yielding five ALF794@h-ZnCPO_x hybrid systems (see ESI). The actual incorporation of the photoCORM into the porous materials was firstly confirmed by IR (Fig. 1). In fact, the characteristic stretching CO bands of ALF794 appear slightly shifted in the loaded matrixes in comparison to the free CORM (e.g. from 1924 and 1859 cm^{-1} , to 1936 and 1868 cm^{-1} for the free ALF794 and the hybrid material ALF794@h-ZnCPO_{0.2}, respectively). This observation seems to be related to the effect of the confinement of the molybdenum complex within the matrix, as previously reported.⁹ Once the successful incorporation of ALF794 into the hierarchical porous matrix h-ZnCPO was confirmed, we evaluated the crystallinity of the resulting materials ALF794@h-ZnCPO_x by XRPD (Fig. S2) and quantified their cargo by elemental analysis (EA), thermogravimetry (TG), and inductively coupled plasma-mass spectrometry (ICP-OES) (see ESI, Fig. S3). Regarding XRPD studies, pristine h-ZnCPO showed wide reflections corroborating the nanometric size of the particles. In addition, the hybrid systems displayed similar XRD patterns than that of the empty matrix, although exhibiting a clear amorphization upon the use of increasing amounts of ALF794 during the synthesis. Noteworthy, the absence of the characteristic reflections of free CORM in the diffractograms discarded its coprecipitation (Fig. S2). On the other hand, concerning the efficiency of the encapsulation process, similar payloads were achieved in all cases (ranging from ~ 0.3 to 0.4 mmol of CORM per g of material), although partial degradation of the Mo complex was observed when higher ratios of ALF794/ Zn^{2+} (x = 0.8, 1) were employed (Table S1, see ESI). Therefore, ALF794@h-ZnCPO_{0.2} which shows the best performance towards the encapsulation of ALF794, achieving a loading of 0.28 mmol of CORM per gram of material and a 97 % of encapsulation efficiency, was selected as the most suitable candidate to further evaluate its properties as a CO-releasing material.

Firstly, ALF794@h-ZnCPO_{0.2} was characterized by high-resolution transmission and scanning electron microscopy (HR-TEM and SEM). As expected, the SEM images confirmed the formation of nanoparticles aggregates with randomly

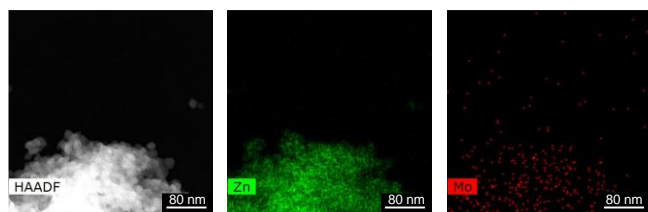


Fig. 2 HR-TEM image and EDX-elemental mapping confirming the incorporation of the CORM (Zn: green, Mo: red).

distributed voids in the mesoporous range (Fig. S4). Furthermore, the elemental mapping of ALF794@h-ZnCPO_0.2 showed the presence of both Zn and Mo in the particles further confirming the loading of the pro-drug (Fig. 2). Regarding the stability of the loaded material, no alteration in XRPD patterns was observed after its incubation in HEPES for 3 hours, although a slight degradation and amorphization occurred after 6 hours (Fig. S5).

Afterwards, the suitability of ALF794@h-ZnCPO_0.2 for the controlled delivery of CO was investigated in simulated physiological conditions (HEPES 10 mM, 37 °C) and compared with the free photoCORM. In particular, the CO releasing rate was followed by the myoglobin assay using UV-vis spectroscopy (see ESI).^{20,21} When kept in the dark, ALF794 does not show spectral changes over 24 h (Fig. S6). In contrast, upon irradiation with UV light ($\lambda = 365$ nm), spectral changes characteristic of CO binding to myoglobin iron center were observed in the Soret band, demonstrating the photoactivation of ALF794. Indeed, ALF794 released 0.95 mmol of CO per mmol of complex after 150 min, which proves the higher lability of one of the three CO ligands per complex. On the other hand, the hybrid system ALF794@h-ZnCPO_0.2 retain the photoactivable properties of free CORM, showing a similar CO kinetic profile ($K \sim 0.01$ mmol CO min⁻¹) and releasing a total amount of 0.33 mmol of CO per mmol of encapsulated CORM after 180 minutes of irradiation (0.09 mmol of CO per g of material) (Fig. 3).

Finally, we evaluated the capacity of h-ZnCPO matrix to trap the Mo fragments into its cavities under physiological conditions (HEPES 10 mM, 37 °C). The results revealed that ca. 83% of the CORMs or iCORMs were kept inside after 6 hours of incubation. This favorable metal retention capacity may be related to the high chemical stability of the porous matrix. Indeed, the Zn leaching accounted only for 9% after incubation

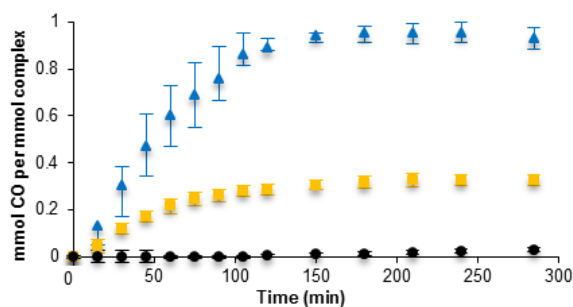


Fig. 3 CO delivery kinetic profiles of free ALF794 (blue triangles) and ALF794@h-ZnCPO_0.2 (orange squares), showing a more controlled CO release than free CORM upon irradiation with UV light. Black circles indicate the CO release profile in darkness for the free CORM.

during the same timeframe and experimental conditions (Table S2). Noteworthy, these results clearly outperform the behavior of the unique CORM@MOF system studied in solution to the date, which completely degraded in physiological medium after 6 hours.¹¹ This achievement may suggest the suitability of MOFs as appropriate platforms for the development of novel and stable CO administration systems in physiological conditions.

In conclusion, we report here for the first time the preparation of a CO releasing material based on a CORM@MOF system by a one-pot strategy. With this aim, we have used the “perturbation-assisted nanofusion method”, yielding a hierarchical h-ZnCPO matrix with textural mesopores ready to encapsulate bulky molecules, such as the CORM ALF794. The optimization of this synthesis-encapsulation methodology has demonstrated that the use of lower CORM/Zn²⁺ ratios leads to more efficient encapsulations. According to the results, ALF794@h-ZnCPO_0.2 has been selected as the most promising candidate. This hybrid system behaves as a photo-CORMA showing a CO delivery rate similar to that of free ALF794. Moreover, the confinement of the CORM molecules into h-ZnCPO allows the protection of the drug towards premature degradation in the physiological medium as well as the retention of most of the potentially toxic decarbonylation fragments. Finally, this study paves the way for the development of new multidrug delivery systems taking advantage of both micro- and mesopores in the carrier, where small bioactive molecules as well as bulkier drugs can be co-encapsulated.

We are grateful for financial support from the Spanish Ministry of Economy and Competitiveness and UE Feder Programs (projects CTQ2014-53486R and CRM Juan de la Cierva contract), University of Granada (CRM Reincorporación Plan Propio), Junta de Andalucía (project P09-FQM-4981 and SR postdoctoral contract), and COST action CM1105. The authors thank Alfama Inc. for providing ALF794. We thank Helia Jeremias and Helena Laronha for the synthesis and purification of ALF794 batches.

Notes and references

- 1 R. Motterlini and L. E. Otterbein, *Nat. Rev. Drug Discov.*, 2010, **9**, 728–743.
- 2 X. Ji, K. Damera, Y. Zheng, B. Yu, L. E. Otterbein and B. Wang, *J. Pharm. Sci.*, 2016, **105**, 406–415.
- 3 U. Schatzschneider, *Br. J. Pharmacol.*, 2015, **172**, 1638–1650.
- 4 C. C. Romão, W. A. Blättler, J. D. Seixas and G. J. L. Bernardes, *Chem. Soc. Rev.*, 2012, **41**, 3571–3583.
- 5 S. García-Gallego and G. J. L. Bernardes, *Angew. Chem. Int. Ed.*, 2014, **53**, 9712–9721.
- 6 S. H. Heinemann, T. Hoshi, M. Westerhausen and A. Schiller, *Chem. Commun.*, 2014, **50**, 3644–3660.
- 7 D. Nguyen and C. Boyer, *ACS Biomater. Sci. Eng.*, 2015, **1**, 895–913.
- 8 A. C. Kautz, P. C. Kunz and C. Janiak, *Dalt. Trans.*, 2016, **45**, 18045–18063.
- 9 M. A. Gonzales, H. Han, A. Moyes, A. Radinos, A. J. Hobbs, N.

- Coombs, S. R. J. Oliver and P. K. Mascharak, *J. Mater. Chem. B*, 2014, **2**, 2107–2113.
- 10 M. Ma, H. Noei, B. Mienert, J. Niesel, E. Bill, M. Muhler, R. A. Fischer, Y. Wang, U. Schatzschneider and N. Metzler-Nolte, *Chem. - A Eur. J.*, 2013, **19**, 6785–6790.
- 11 F. J. Carmona, S. Rojas, P. Sánchez, H. Jeremias, A. R. Marques, C. C. Romão, D. Choquesillo-Lazarte, J. A. R. Navarro, C. R. Maldonado and E. Barea, *Inorg. Chem.*, 2016, **55**, 6525–6531.
- 12 S. Diring, A. Carné-Sánchez, J. Zhang, S. Ikemura, C. Kim, H. Inaba, S. Kitagawa and S. Furukawa, *Chem. Sci.*, 2016, **8**, 2381–2386.
- 13 A. R. Marques, L. Kromer, D. J. Gallo, N. Penacho, S. S. Rodrigues, J. D. Seixas, G. J. L. Bernardes, P. M. Reis, S. L. Otterbein, R. A. Ruggieri, A. S. G. Gonçalves, A. M. L. Gonçalves, M. N. De Matos, I. Bento, L. E. Otterbein, W. A. Blättler and C. C. Romão, *Organometallics*, 2012, **31**, 5810–5822.
- 14 Y. Yue, Z.-A. Qiao, P. F. Fulvio, A. J. Binder, C. Tian, J. Chen, K. M. Nelson, X. Zhu and S. Dai, *J. Am. Chem. Soc.*, 2013, **135**, 9572–9575.
- 15 S. Rojas, T. Devic and P. Horcajada, *J. Mater. Chem. B*, 2017, **5**, 2560–2573.
- 16 H. Deng, S. Grunder, K. E. Cordova, C. Valente, H. Furukawa, M. Hmadeh, F. Gándara, A. C. Whalley, Z. Liu, S. Asahina, Hi. Kazumori, M. O’Keeffe, O. Terasaki, J. F. Stoddart and O. M. Yaghi, *Science*, 2012, **336**, 1018–1023.
- 17 Y. Yue, P. F. Fulvio and S. Dai, *Acc. Chem. Res.*, 2015, **48**, 3044–3052.
- 18 I. Imaz, M. Rubio-Martínez, L. García-Fernández, F. García, D. Ruiz-Molina, J. Hernando, V. Puentes and D. Maspoch, *Chem. Commun.*, 2010, **46**, 4737.
- 19 H. Zheng, Y. Zhang, L. Liu, W. Wan, P. Guo, A. M. Nystrom and X. Zou, *J. Am. Chem. Soc.*, 2016, 962–968.
- 20 R. Motterlini, J. E. Clark, R. Foresti, P. Sarathchandra, B. E. Mann and C. J. Green, *Circ. Res.*, 2002, **90**, e17–e24.
- 21 D. E. Bikiel, E. González Solveyra, F. Di Salvo, H. M. S. Milagre, M. N. Eberlin, R. S. Corrêa, J. Ellena, D. A. Estrin and F. Doctorovich, *Inorg. Chem.*, 2011, **50**, 2334–2345.